Supplementary materials for

Multi-omics analysis identifies novels genes involved in glioma prognosis

This file includes:

Supplementary figures 2
- Figure S1: Weighted gene co-expression network analysis 2
- Figure S2: Tumor mutation burden in the GBM and LGG cohorts. 3
- Figure S3. Mutations and DNA methylation state relating to the prognosis of gliomas. 3
- Figure S4: Kaplan–Meier estimates of overall survival between GBM patients with wild type IDH1 and GBM patients with mutant type IDH1. 4
- Figure S5: Analysis of the multi-layer factors relevant to prognosis of glioma patients in the CGGA independent validation cohort. 5
- Figure S6: Statistical overlap between the 178 meGenes with cell-type specific markers are depicted according to Benjamini-Hochberg corrected p-values. 5
- Figure S7: A schematic overview of the multi-layered computational procedure. 6
- Figure S8: Results of multivariate Cox proportional hazards analysis for the IDH1 wild type patients. 6

Supplementary tables 7
- Table S1: Data and characteristics of the TCGA sample set 7
- Table S2: The 17 grade-related genes are associated with outcome of cancers. 8
- Table S3: Co-active grade-related genes and meGenes in the turquoise WGCNA module. 9
- Table S4: Co-active grade-related genes and meGenes in the grey WGCNA module 14
- Table S5: Sample size according to IDH1 and PTEN gene mutation, histological grading and activity states of the 178 meGenes 15
- Table S6: Supporting evidences for the 178 meGenes from publications in PubMed. 16
- Table S7: Characteristics of the IDH1 wild type sample set. 20

References 21

Supplementary figures

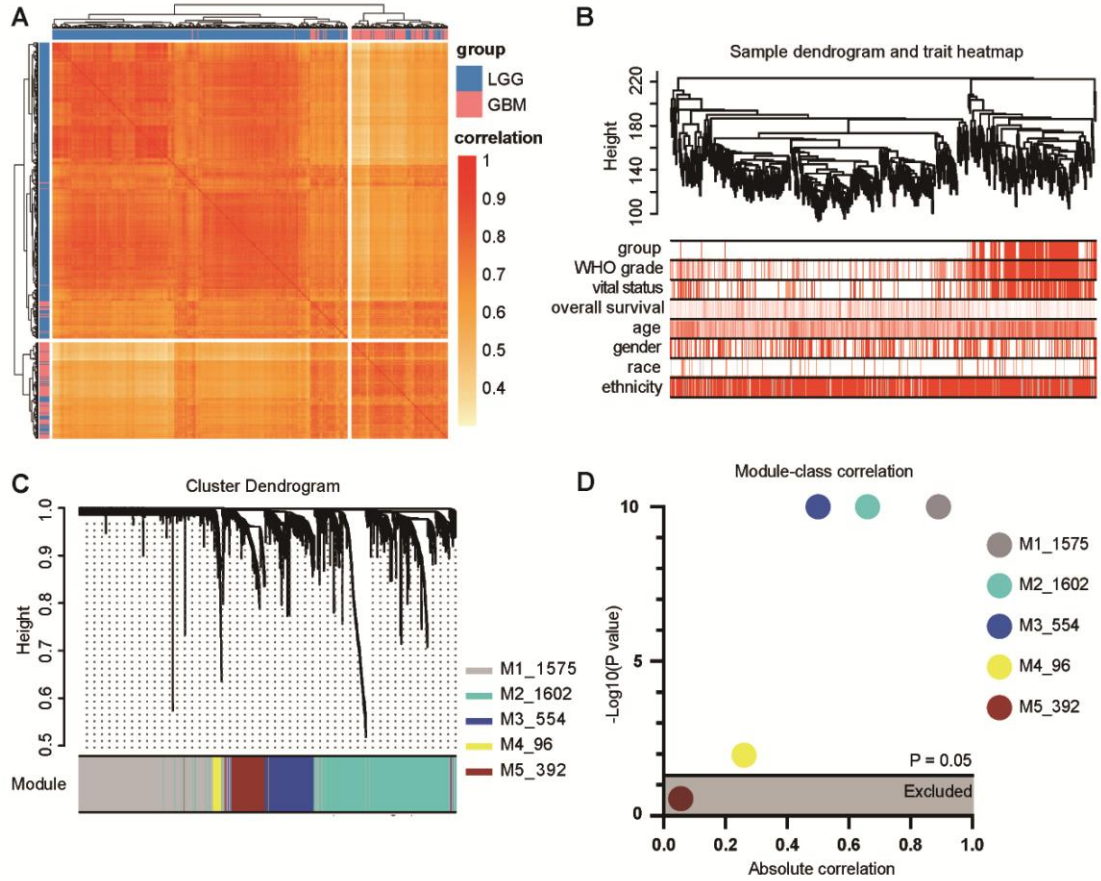

Figure S1: Weighted gene co-expression network analysis

(**A**) The Spearman correlation matrix heatmap indicating extent of similarity between samples in the expression profiles of DEGs identified between LGG and GBM. (**B**) Sample dendrogram and trait heatmap. Each branch indicates a single sample. (**C**) Hierarchical clustering presenting five modules having co-expressed genes. The color bars below give information on module membership, the number after the module name depicts the total number of genes in the module. (**D**) Correlation analysis showing that four modules are strongly correlated with the clinical traits. Spearman correlations between scc_GT and scc_GM were calculated for each gene in each module, where scc_GT is the Spearman correlation coefficient between genes' expression profile and the clinical traits and scc_GM is the Spearman correlation coefficients between gene's expression profile and the module eigengene.

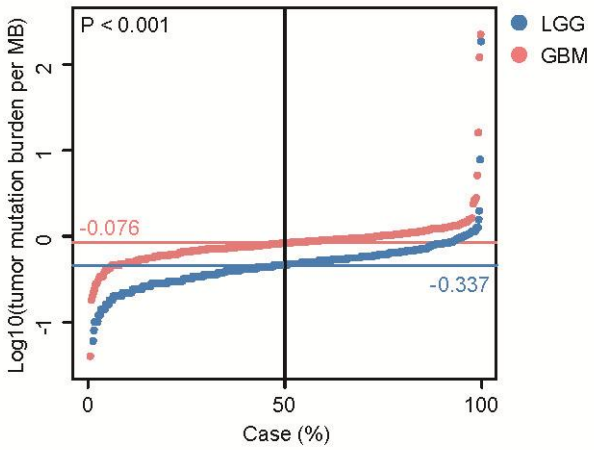

Figure S2: Tumor mutation burden in the GBM and LGG cohorts.

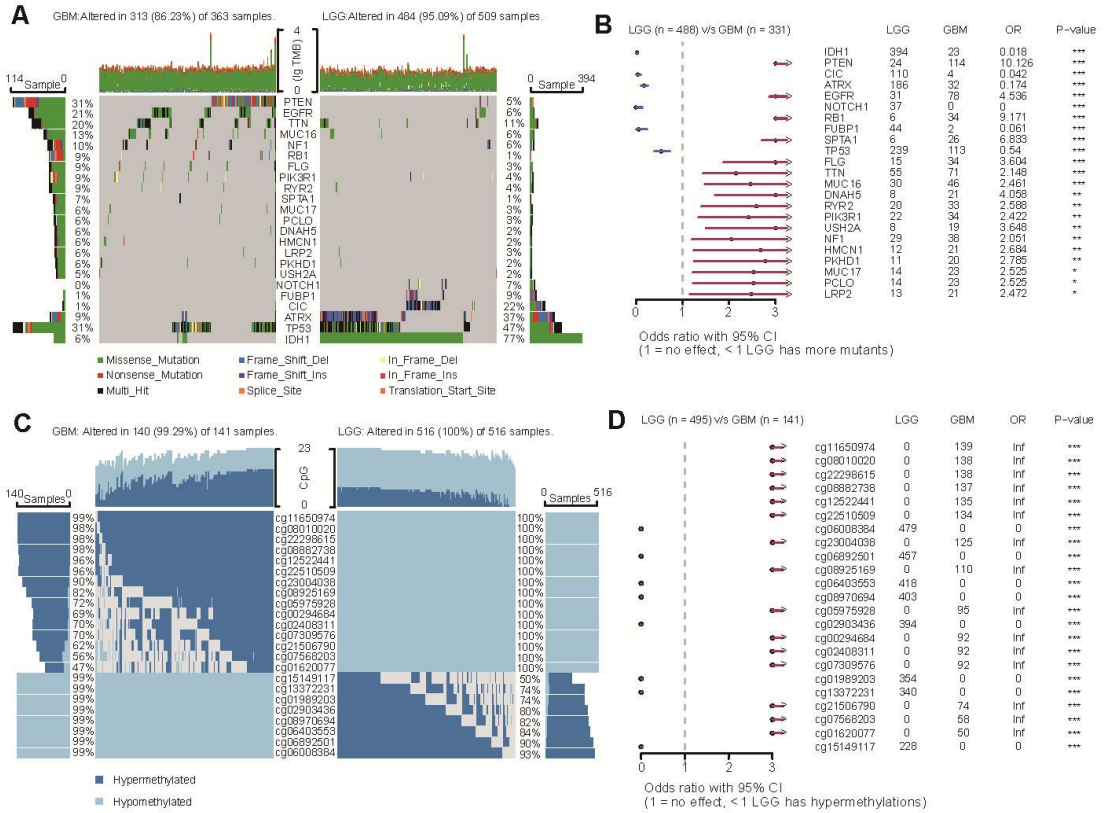

Figure S3. Mutations and DNA methylation state relating to the prognosis of gliomas.

(**A**) Oncoprint of genes that are most frequently altered in GBM or LGG cohorts. Samples are ordered by nonsynonymous mutational load. Frequency of mutated samples as percentage of the total number of samples is shown on the left side of the plot for GBM cohort and on the right side for LGG cohort. Genes with a mutation frequency ≥5% either in GBM cohort or LGG cohort are included in the oncoprint. (**B**) Forest plot with odds ratio (OR) markers for the genes differentially mutated in GBM and LGG cohorts. Fisher exact test was used to examine the significances of associations between mutation frequency and glioma subtypes. Genes are sorted top to bottom by smallest to largest OR. * P value < 0.05, ** P value < 0.01, *** P value < 0.001. Error bar indicating 95% CI of the OR. (**C**) Waterfall plot showing the frequency of hypermethylated

(methylation level >0.8) and hypomethylated (methylation level <0.2) CpG islands in 4 grade-related genes in the comparison between GBM and LGG cohorts. CpGs are ordered by the frequency, which is shown on the left side of the plot for GBM cohort and on the right side for LGG cohort. Samples are clustered by the methylation pattern, and fractions of hypermethylated and hypomethylated CpGs are shown on the top of the plot. Hypermethylated CpGs are labeled in dark blue, hypomethylated in light blue. (**D**) Forest plot with OR markers for the CpGs in hyper- or hypo- methylaiton state in the comparison between GBM and LGG cohorts. Fisher exact test was used to examine the significances of associations between methylation state and histological grades. Regions are sorted top to bottom by smallest to largest OR. * P value < 0.05, ** P value < 0.01, *** P value < 0.001. Error bar indicating 95% CI of the OR.

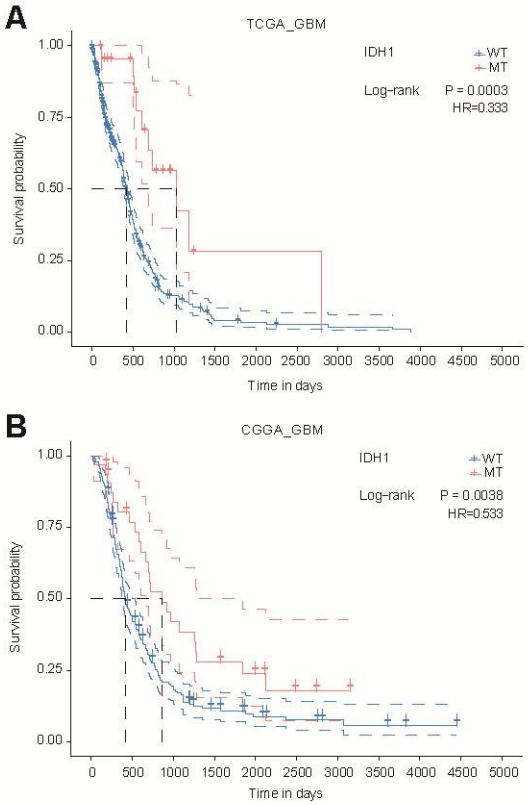

Figure S4: Kaplan–Meier estimates of overall survival between GBM patients with wild type IDH1 and GBM patients with mutant type IDH1.

Kaplan-Meier survival curves between the GBM patient groups subdivided by IDH1 genetic states in the TCGA set (**A**) and CGGA independent validation set (**B**). WT: wild type, MT: mutant type. Logrank tests were used to examine the significances of differences.

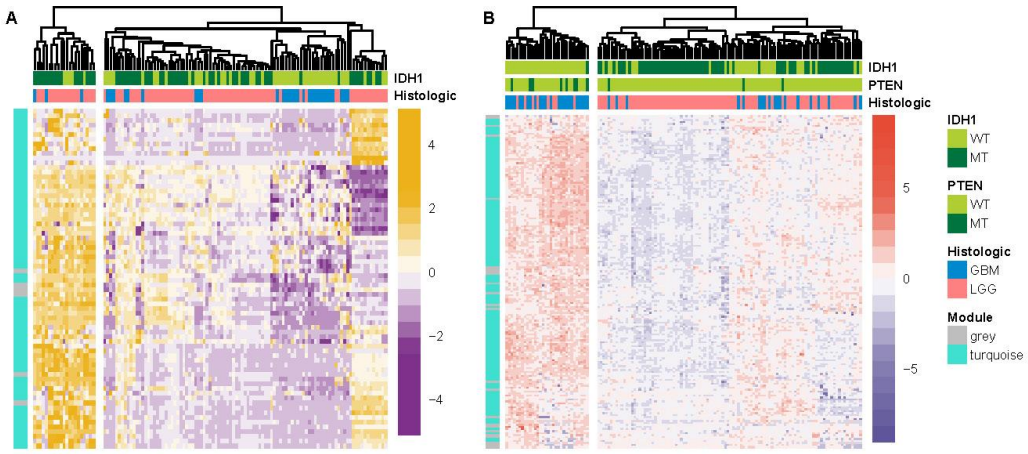

Figure S5: Analysis of the multi-layer factors relevant to prognosis of glioma patients in the CGGA independent validation cohort.

(**A**) Unsupervised clustering of the DNA methylation profile of CpGs in the 178 meGenes. The top two rows indicate IDH1 mutation state and histologic grades, *i.e.*, LGG and GBM. (**B**) Unsupervised clustering of the expression profile of the 178 meGenes. The top three rows indicate IDH1 and PTEN mutation state, and histologic grades, *i.e.*, LGG and GBM.

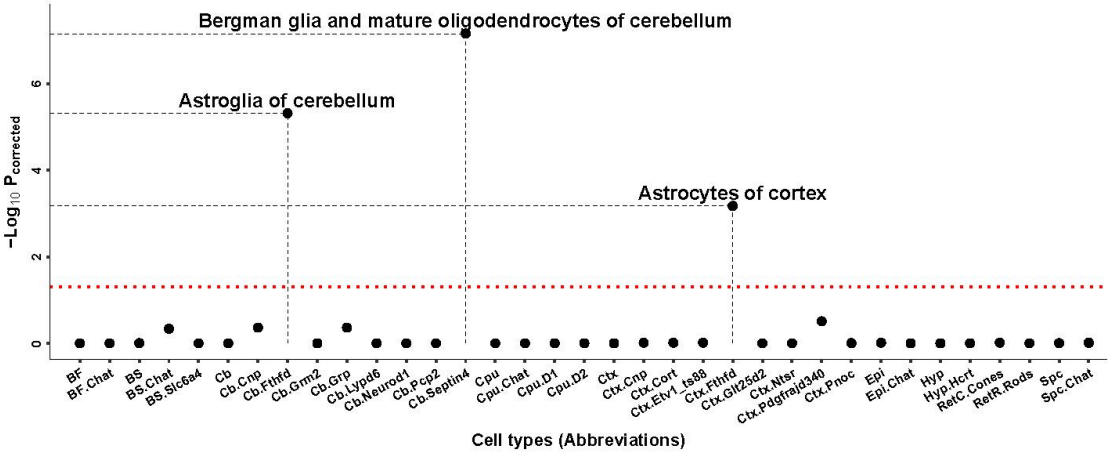

Figure S6: Statistical overlap between the 178 meGenes with cell-type specific markers are depicted according to Benjamini-Hochberg corrected p-values.

The red dotted line indicates the significant threshold.

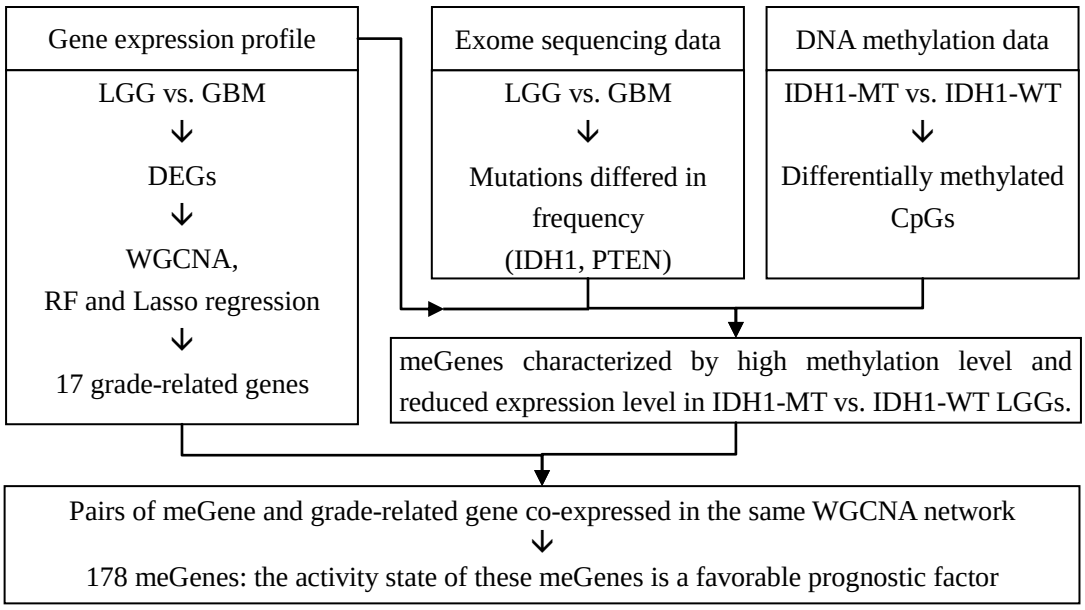

Figure S7: A schematic overview of the multi-layered computational procedure.

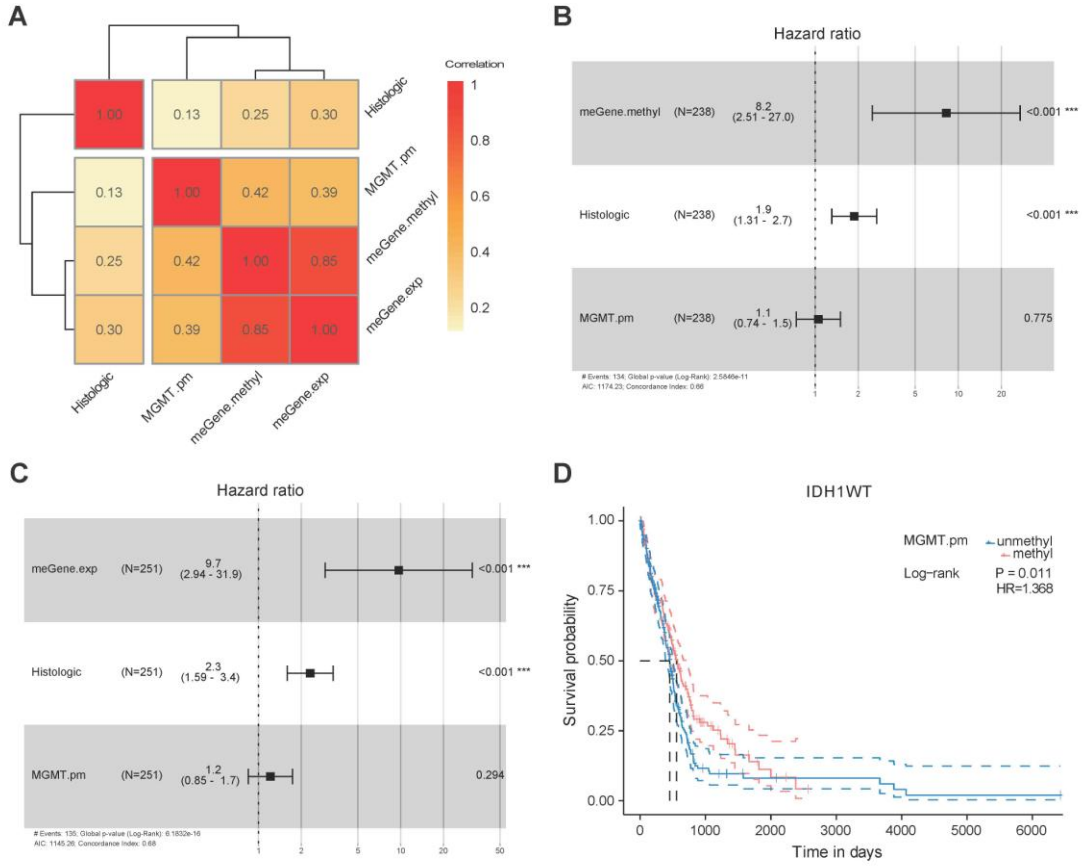

Figure S8: Results of multivariate Cox proportional hazards analysis for the IDH1 wild type patients.

(**A**) Expression level of the 178 meGenes was highly correlated with DNA methylation level. (**B, C**) Multivariate Cox regression analysis was performed to evaluate overall survival based on histologic grade, MGMT promoter methylation status together with DNA methylation level of the 178 meGenes (**B**), and together with expression level of the 178 meGenes (**C**). Hazard ratio, 95%

95% confidence interval (in parentheses) and P value were shown. * P value < 0.05, ** P value < 0.01, *** P value < 0.001. (D) Kaplan–Meier estimates of overall survival between IDH1 wild type patients subdivided by MGMT promoter methylation status. Logrank tests were used to examine the significances of differences.

Supplementary tables

Table S1: Data and characteristics of the TCGA sample set

	GBM	LGG	P value (GBM vs LGG)
Data category	Number of samples	Number of samples	
WXS*	363	507	
RNA-seq	146	505	
Methylation array	134	507	
Total number of samples	369	516	
Characteristic			
Age at diagnosis	60.262 ±0.704	42.942 ±0.588	<0.001[a]
Gender			0.026[b]
Male	230(62.3%)	285 (55.2%)	
Female	136 (36.9%)	230 (44.6%)	
Not reported	3(0.81%)	1(0.19%)	
WHO grade			<0.001[b]
Ⅱ	0 (0%)	307 (59.5%)	
Ⅲ	0 (0%)	208 (40.31%)	
Ⅳ	366 (99.2%)	0 (0%)	
Not reported	3(0.8%)	1(0.2%)	
Race			0.001[b]
White	314 (85.1%)	475 (92.1%)	
Other	44 (11.9%)	30 (5.8%)	
Not reported	11 (2.9%)	11 (2.1%)	
Ethnicity			0.002[b]
Not hispanic or latino	292 (79.1%)	449 (87.0%)	
Hispanic or latino	5 (1.4%)	32 (6.2%)	
Not reported	72 (19.5%)	35 (6.8%)	
Vital status			<0.001[b]
Alive	85 (23.0%)	388 (75.2%)	
Dead	280 (75.9%)	125 (24.2%)	
Not reported	4(1.1%)	3(0.6%)	
Overall survival (day)	448	2660	<0.001[c]
	95%CI=399-485	95%CI=2052-3470	

[a], t tests; [b], Chi-square test; [c], Logrank test

* WXS: whole exome sequencing data

Table S2: The 17 grade-related genes are associated with outcome of cancers.

Gene	Effect	Disease	References	WGCNA module	*Exp.
H2BC12L	High H2BC12 expression is associated with a poor survival outcome of LGGs.	Gliomas	(ZHOU *et al.* 2022)	Grey	Down
HBG1	Hemoglobin level was found to be associated with overall survival of glioma patients.	Gliomas	(KAISMAN-ELBAZ *et al.* 2020)	Grey	Down
HBG2	Hemoglobin level was found to be associated with overall survival of glioma patients.	Gliomas	(KAISMAN-ELBAZ *et al.* 2020)	Grey	Down
EIF3CL	Expression of EIF3CL has been reported to be essential for glioma survival.	Gliomas	(CHEN *et al.* 2020)	Turquoise	Down
H3-3A	High H3-3A expression is linked to molecular alterations found in LGGs.	Gliomas	(HERVÁS-CORPIÓN *et al.* 2021)	Turquoise	Down
NET1	High NET1 expression is associated with better survival of glioma patients.	Gliomas	(KIM *et al.* 2013)	Turquoise	Up
PPIA	High PPIA expression is associated with poor survival of glioma patients.	Gliomas	(WANG *et al.* 2019)	Turquoise	Down
SELENOH	SELENOH expression is positively correlated with SEPHS2 which is an independent prognostic factor for LGG.	Gliomas	(ZHANG *et al.* 2021)	Turquoise	Down
UQCRHL	UQCRHL is the paralog of UQCRH which is associated with survival rates of patients with hepatocellular carcinoma.	Hepatocellular carcinoma	(PARK *et al.* 2017)	Turquoise	Down
GUCA2A	High GUCA2A expression is associated with a better overall survival of colorectal cancer patients.	Colorectal cancer	(CAO *et al.* 2022)	Grey	Down
POTEG	Low POTEG expression is associated with poor survival of patients with esophageal squamous cell carcinoma.	Esophageal squamous cell carcinoma	(WANG *et al.* 2018)	Grey	Down
NPIPB5	Expression of NPIPB5 is relevant to survival rates of clear cell renal cell carcinoma.	Clear cell renal cell carcinoma	(WANG *et al.* 2022)	Turquoise	Down
POTEE	High POTEE expression is associated with poor survival of patients with colorectal cancer.	Colorectal cancer	(SHEN *et al.* 2019)	Turquoise	Down
FKBP1C	High FKBP1A expression is correlated with a poor survival rate in LIHC patients.	Liver hepatocellular carcinoma	(Li et al. 2022)	Turquoise	Down
PGK2	High PGK1 expression of is associated with poor survival of cancer patients.	Cancer	(ZHANG *et al.* 2023)	Grey	Down
PPIAL4E	Known as COAS2. COAS2 was over-expressed almost exclusively in aggressive metastatic or chemotherapy resistant tumors.	Aggressive metastatic tumors	(Meza-Zepeda et al. 2002)	Grey	Down
RHAG	Reactions catalyzed by RHAG are core exclusively in cancer.	Cancer	(Gatto et al. 2020)	Grey	Down

*Exp.: change of expression level in LGG cohort relative to GBM corhort.

Table S3: Co-active grade-related genes and meGenes in the turquoise WGCNA module.

Grade-related gene	meGene	NO. methylated CpGs ¶	Expression correlation*	
			Correlation coefficient	P value
FKBP1C	ARAP3	13	0.280334	8.99E-11
FKBP1C	PABPC1L	1	0.281643	7.29E-11
FKBP1C	GRB14	3	0.281756	7.16E-11
FKBP1C	PDGFA	11	0.281811	7.1E-11
FKBP1C	WEE1	2	0.290715	1.65E-11
FKBP1C	ABRACL	7	0.293377	1.06E-11
FKBP1C	CD151	1	0.304069	1.69E-12
FKBP1C	BEST4	6	0.304396	1.59E-12
FKBP1C	OCIAD2	7	0.305952	1.21E-12
FKBP1C	AP1S3	1	0.306585	1.08E-12
FKBP1C	TIMP1	2	0.309988	5.9E-13
FKBP1C	ZYX	3	0.31364	3.05E-13
FKBP1C	FAM20C	7	0.320042	9.4E-14
FKBP1C	PCOLCE	2	0.324534	4.04E-14
FKBP1C	PTGFRN	6	0.325473	3.38E-14
FKBP1C	COL5A2	1	0.329089	1.69E-14
FKBP1C	IGFBP2	4	0.333529	7.15E-15
FKBP1C	VAV3	1	0.344843	7.45E-16
FKBP1C	TTYH3	13	0.394824	1.07E-20
H3-3A	S100A13	10	-0.35941	3.52E-17
H3-3A	ECHDC2	3	-0.3495	2.86E-16
H3-3A	RARRES2	4	-0.33102	1.17E-14
H3-3A	ADAM33	5	-0.31623	1.9E-13
H3-3A	RBM47	2	0.279905	9.63E-11
H3-3A	LAPTM5	5	0.279913	9.62E-11
H3-3A	CYTL1	4	0.280394	8.91E-11
H3-3A	MMP14	8	0.286824	3.15E-11
H3-3A	SLFN12	2	0.287564	2.79E-11
H3-3A	TMEM154	3	0.294682	8.5E-12
H3-3A	TMEM106C	1	0.296272	6.49E-12
H3-3A	RUNX1	7	0.301088	2.84E-12
H3-3A	SLC7A7	2	0.302881	2.08E-12
H3-3A	TENT5A	5	0.303114	1.99E-12
H3-3A	CNN3	1	0.315581	2.14E-13
H3-3A	COLGALT1	1	0.31707	1.63E-13
H3-3A	GAL3ST4	4	0.327447	2.32E-14
H3-3A	CASP5	1	0.330744	1.23E-14
H3-3A	MSR1	3	0.334525	5.88E-15
H3-3A	PARP9	1	0.34195	1.34E-15
H3-3A	ZNF217	4	0.344664	7.72E-16

H3-3A	MYD88	8	0.34614	5.71E-16
H3-3A	LAMC1	1	0.346454	5.36E-16
H3-3A	CALD1	5	0.354621	9.78E-17
H3-3A	RAB42	2	0.356333	6.81E-17
H3-3A	RCAN1	4	0.36855	4.79E-18
H3-3A	MMP2	3	0.378455	5.13E-19
H3-3A	CRISPLD1	1	0.384256	1.33E-19
H3-3A	PSPH	1	0.38878	4.59E-20
H3-3A	AK2	3	0.397665	5.36E-21
H3-3A	WEE1	2	0.400658	2.56E-21
H3-3A	PDIA4	1	0.425786	3.87E-24
H3-3A	BTG3	3	0.465081	4.7E-29
H3-3A	GINS4	1	0.470687	8.27E-30
H3-3A	FNDC3B	9	0.474362	2.6E-30
H3-3A	GPX7	2	0.47799	8.19E-31
H3-3A	CASP3	1	0.517935	9.33E-37
H3-3A	ERI1	6	0.524221	9.14E-38
NET1	BEST4	6	-0.41348	9.98E-23
NET1	VASN	7	-0.3998	3.17E-21
NET1	SLC2A4RG	5	-0.38459	0
NET1	TNFRSF12A	6	-0.38361	1.55E-19
NET1	UPP1	14	-0.38228	2.11E-19
NET1	G0S2	10	-0.37838	5.21E-19
NET1	FAM20C	7	-0.37305	1.75E-18
NET1	CLCF1	14	-0.36781	5.65E-18
NET1	RGS16	12	-0.36126	1.39E-17
NET1	PDIA4	1	-0.36056	1.76E-17
NET1	TIMP1	2	-0.35707	4.97E-17
NET1	FABP5	6	-0.35559	7.98E-17
NET1	GALNT3	7	-0.3506	2.27E-16
NET1	ZYX	3	-0.34825	4.34E-16
NET1	PCOLCE	2	-0.3482	3.74E-16
NET1	FGFRL1	26	-0.34815	3.77E-16
NET1	TRIP6	8	-0.3479	4.69E-16
NET1	AP1S3	1	-0.34579	6.13E-16
NET1	NNMT	1	-0.34499	7.22E-16
NET1	ZDHHC12	3	-0.33974	2.72E-15
NET1	SAA1	1	-0.33876	2.54E-15
NET1	EMP3	6	-0.33808	3.83E-15
NET1	FAM181A	5	-0.33295	8E-15
NET1	PTX3	1	-0.33285	8.16E-15
NET1	PPM1M	10	-0.32876	2.43E-14
NET1	STEAP3	10	-0.32751	2.29E-14

NET1	PSRC1	2	-0.32584	4.26E-14
NET1	ANKRD53	7	-0.32565	3.27E-14
NET1	FKBP10	5	-0.3256	4.46E-14
NET1	C3orf52	2	-0.32504	3.67E-14
NET1	PABPC1L	1	-0.32249	5.95E-14
NET1	GPR157	3	-0.32073	8.26E-14
NET1	COLGALT1	1	-0.32021	1.22E-13
NET1	PLOD3	1	-0.31918	1.48E-13
NET1	IGFLR1	1	-0.31863	1.22E-13
NET1	DOK3	5	-0.31814	1.79E-13
NET1	ADAM12	18	-0.31777	1.43E-13
NET1	CD151	1	-0.31735	2.07E-13
NET1	MYBPH	2	-0.31581	2.06E-13
NET1	TTYH3	13	-0.31573	2.78E-13
NET1	F2RL2	1	-0.3148	2.47E-13
NET1	PYGL	9	-0.31447	2.62E-13
NET1	MCUB	2	-0.31439	2.66E-13
NET1	CA3	8	-0.31422	2.75E-13
NET1	PDGFA	11	-0.31384	2.94E-13
NET1	EMILIN1	2	-0.31247	3.78E-13
NET1	CASP6	4	-0.31097	4.95E-13
NET1	TEAD3	4	-0.31001	5.89E-13
NET1	PDPN	13	-0.30935	8.67E-13
NET1	PLK3	1	-0.3093	6.68E-13
NET1	TUBA1C	9	-0.30859	7.58E-13
NET1	CD63	2	-0.30757	1.19E-12
NET1	LAMB4	1	-0.30659	1.08E-12
NET1	SOCS1	3	-0.30585	1.23E-12
NET1	HOXC10	2	-0.30547	1.32E-12
NET1	RAB42	2	-0.3054	1.33E-12
NET1	AEBP1	10	-0.30384	2.27E-12
NET1	DIRAS3	2	-0.30174	2.53E-12
NET1	CTF1	3	-0.29949	3.74E-12
NET1	EFEMP2	6	-0.29882	5.35E-12
NET1	CLIC1	14	-0.29872	5.43E-12
NET1	TGIF1	17	-0.29814	4.72E-12
NET1	HDHD3	1	-0.2981	6.03E-12
NET1	ARL9	7	-0.29782	4.98E-12
NET1	PINLYP	1	-0.29724	5.5E-12
NET1	DCTD	8	-0.29534	9.58E-12
NET1	ABCC3	4	-0.29516	7.84E-12
NET1	S100A16	3	-0.29451	1.1E-11
NET1	RINL	6	-0.29437	8.96E-12

NET1	CARD19	7	-0.29419	1.16E-11
NET1	TCIRG1	12	-0.29234	1.57E-11
NET1	CHI3L1	5	-0.29224	1.28E-11
NET1	TPRG1	4	-0.2919	1.36E-11
NET1	ECHDC2	3	-0.29186	1.37E-11
NET1	FAM114A1	4	-0.2916	1.78E-11
NET1	B3GNT7	9	-0.29128	1.51E-11
NET1	MRC2	6	-0.29098	1.97E-11
NET1	METTL7B	1	-0.29017	2.25E-11
NET1	OTP	3	-0.28919	2.13E-11
NET1	PTGFRN	6	-0.28749	3.48E-11
NET1	F3	4	-0.28704	3.73E-11
NET1	ALDH3A1	6	-0.28642	3.36E-11
NET1	SLC43A3	4	-0.28565	3.81E-11
NET1	FCHSD1	8	-0.28561	3.83E-11
NET1	TMEM106C	1	-0.28554	4.76E-11
NET1	RUBCNL	8	-0.28395	5.02E-11
NET1	SLC16A3	22	-0.28383	5.12E-11
NET1	WEE1	2	-0.2837	6.38E-11
NET1	ABRACL	7	-0.28334	5.55E-11
NET1	CAPG	8	-0.28267	6.18E-11
NET1	PTPN7	4	-0.28094	8.16E-11
NET1	PRICKLE3	7	-0.28	9.48E-11
NPIPB5	LAMB4	1	0.30405	1.69E-12
NPIPB5	NFE2L3	2	0.312202	3.96E-13
NPIPB5	ADAMTSL4	5	0.342123	1.29E-15
NPIPB5	RDH5	6	0.356646	6.37E-17
NPIPB5	AVIL	2	0.364513	1.17E-17
NPIPB5	PABPC1L	1	0.37012	3.38E-18
PPIA	CLIC1	14	0.286159	4.31E-11
PPIA	ETV2	6	0.289234	2.11E-11
PPIA	HEBP2	3	0.290402	1.74E-11
PPIA	GAL3ST4	4	0.292997	1.41E-11
PPIA	PABPC1L	1	0.293213	1.09E-11
PPIA	IGF2BP3	7	0.293451	1.05E-11
PPIA	GRB14	3	0.294576	8.65E-12
PPIA	TIMP1	2	0.297453	6.73E-12
PPIA	COL6A1	1	0.297903	6.24E-12
PPIA	PDGFA	11	0.298512	4.42E-12
PPIA	TUBA1C	9	0.303648	1.82E-12
PPIA	LAMC1	1	0.31043	7.17E-13
PPIA	ENPP1	3	0.3121	4.04E-13
PPIA	ELN	5	0.313592	3.08E-13

PPIA	ADGRE5	2	0.313977	2.87E-13
PPIA	VAV3	1	0.316566	1.79E-13
PPIA	FNDC3B	9	0.321193	7.58E-14
PPIA	DNAH11	4	0.325532	3.34E-14
PPIA	CASP6	4	0.325572	3.32E-14
PPIA	MYD88	8	0.326822	3.53E-14
PPIA	MCUB	2	0.329192	1.66E-14
PPIA	SLC43A3	4	0.33716	3.49E-15
PPIA	BCAT1	15	0.347273	4.53E-16
PPIA	CD63	2	0.348115	4.47E-16
PPIA	FKBP10	5	0.352078	1.78E-16
PPIA	CRISPLD1	1	0.352381	1.65E-16
PPIA	ITPRIPL1	8	0.355707	7.77E-17
PPIA	IGFBP2	4	0.357276	4.69E-17
PPIA	COL5A2	1	0.357466	5.35E-17
PPIA	PCOLCE	2	0.359694	3.32E-17
PPIA	ADAM12	18	0.363302	1.52E-17
PPIA	RAB42	2	0.366913	6.89E-18
PPIA	DPY19L1	1	0.37118	0
PPIA	ABRACL	7	0.376576	7.88E-19
PPIA	GINS4	1	0.378989	4.53E-19
PPIA	COLGALT1	1	0.382826	0
PPIA	PTX3	1	0.384019	1.41E-19
PPIA	HEXB	10	0.389813	3.59E-20
PPIA	BTG3	3	0.391529	0
PPIA	CD151	1	0.400066	0
PPIA	ERI1	6	0.402165	0
PPIA	GPX7	2	0.410172	0
PPIA	ZYX	3	0.414777	0
PPIA	CASP3	1	0.419129	0
PPIA	TMEM106C	1	0.424732	0
PPIA	MMP2	3	0.432446	0
PPIA	RCAN1	4	0.432528	6.15E-25
PPIA	PTGFRN	6	0.436038	0
PPIA	TTYH3	13	0.44601	0
PPIA	WEE1	2	0.447767	0
PPIA	PLOD3	1	0.452664	0
PPIA	FAM20C	7	0.484047	1.15E-31
PPIA	PDIA4	1	0.502773	0
PPIA	PSPH	1	0.524558	0
SELENOH	CLCF1	14	0.292049	1.32E-11
SELENOH	EMILIN1	2	0.311103	4.83E-13
SELENOH	IGFLR1	1	0.319736	9.95E-14

SELENOH	ELN	5	0.338931	2.46E-15
SELENOH	TCIRG1	12	0.341804	1.38E-15
SELENOH	SLC2A4RG	5	0.347499	4.32E-16
SELENOH	ZYX	3	0.35115	2.03E-16
SELENOH	PCOLCE	2	0.361846	2.08E-17
SELENOH	ANKRD53	7	0.363	1.62E-17
SELENOH	ARPC1B	10	0.384115	1.38E-19
SELENOH	PLOD3	1	0.394542	1.15E-20
SELENOH	CD151	1	0.404783	9.16E-22
SELENOH	COL6A1	1	0.409583	2.72E-22
SELENOH	COLGALT1	1	0.433007	5.39E-25
SELENOH	FAM20C	7	0.44948	5.02E-27
SELENOH	PABPC1L	1	0.474089	2.84E-30
UQCRHL	BANK1	6	-0.28756	2.79E-11
UQCRHL	CA3	8	0.280275	9.08E-11
UQCRHL	GPX7	2	0.28577	3.74E-11
UQCRHL	RHOC	2	0.294429	8.87E-12
UQCRHL	LAMB4	1	0.299791	3.55E-12
UQCRHL	CD72	1	0.318891	1.16E-13
UQCRHL	TCIRG1	12	0.341241	1.55E-15
UQCRHL	SLC2A4RG	5	0.342754	1.14E-15
UQCRHL	ARPC1B	10	0.355237	8.59E-17
UQCRHL	AK2	3	0.357864	4.91E-17
UQCRHL	IGFLR1	1	0.370853	2.87E-18
UQCRHL	ANKRD53	7	0.391686	2.29E-20

[¶] In the body of the meGene, total number of CpGs highly methylated in IDH1 mutant LGG samples. [*] Based on the similarity of expression patterns across the LGG samples, the Spearman correlations were calculated for each pair of meGene and grade-related gene, which were co-expressed in the turquoise WGCNA module. A co-expression threshold p-value of 10^{-10} was used to eliminate weak connections.

Table S4: Co-active grade-related genes and meGenes in the grey WGCNA module

Grade-related gene	meGene	NO. methylated CpGs [¶]	Expression correlation[*]	
			Correlation coefficient	P value
GUCA2A	AQP1	7	-0.11182	0.011029
GUCA2A	TGM5	5	-0.09368	0.03337
GUCA2A	CNGA3	13	-0.09332	0.034069
GUCA2A	SMO	5	0.093026	0.034634
GUCA2A	SIX2	8	0.157338	0.000334
H2BC12L	MGARP	7	-0.08875	0.043897
H2BC12L	ADGRD2	3	0.10333	0.018885
H2BC12L	KCTD19	2	0.108326	0.013818
H2BC12L	FEZF1	10	0.118276	0.007153

HBG1	BANF2	2	0.088897	0.043544
HBG1	SLC28A1	1	0.093846	0.033063
HBG2	EGFR	35	-0.12611	0.004116
HBG2	SMO	5	-0.09053	0.039818
PGK2	FAM221A	8	-0.09254	0.035605
PGK2	WNT16	5	0.136679	0.001859
POTEG	CNGA3	13	0.091703	0.037304
POTEG	TGM5	5	0.092387	0.035903
POTEG	FZD7	3	0.098968	0.024564
POTEG	RIPOR3	1	0.107059	0.014974
POTEG	PLSCR2	1	0.108973	0.013258
POTEG	FAM221A	8	0.111054	0.011591
POTEG	ESPNL	10	0.111902	0.010967
POTEG	SMO	5	0.113942	0.009586
POTEG	CDC42BPG	3	0.119573	0.006541
POTEG	OCSTAMP	6	0.121479	0.005727
POTEG	KCTD19	2	0.128374	0.003488
POTEG	AGBL2	1	0.134108	0.002267
PPIAL4E	CDC42BPG	3	-0.12117	0.005852
PPIAL4E	RASSF10	12	-0.11357	0.009826
PPIAL4E	EN2	3	-0.10276	0.01956
PPIAL4E	ACOT12	4	-0.0949	0.03113
RHAG	VOPP1	12	0.091126	0.038521
RHAG	CFAP77	6	0.094102	0.032586
RHAG	BANF2	2	0.094348	0.032132
RHAG	MAB21L2	6	0.097521	0.026749
RHAG	SMO	5	0.102574	0.019778
RHAG	FOXJ1	6	0.113213	0.01006
RHAG	ESPNL	10	0.125467	0.004311

[¶] In the body of the meGene, total number of highly methylated CpGs in IDH1 mutant LGG samples. [*] Based on the similarity of expression patterns across the LGG samples, the Spearman correlations were calculated for each pair of meGene and grade-related gene, which were co-expressed in the grey WGCNA module.

Table S5: Sample size according to IDH1 and PTEN gene mutation, histological grading and activity states of the 178 meGenes

178 meGenes		IDH1-WT	IDH1-MT	PTEN-WT	PTEN-MT	LGG	GBM
Active	Highly expressed	221	27	184	64	104	144
	Lowly methylated	213	0	151	62	87	126
Inactive	Lowly expressed	30	373	398	5	401	2
	Highly methylated	27	401	422	6	420	8

Table S6: Supporting evidences for the 178 meGenes from publications in PubMed.

Gene symbol	PMID	WGCNA module
FZD7	38816349,31419987,30010402,28481871,27852064	grey
METTL7B	37543576,38952353,35769464,37151605,37543576	turquoise
CD151	22926763,26992919,22495828,16204036	turquoise
VAV3	36539408,36960857,32894375,19008376	turquoise
CASP6	36778205,36119521,34861452,34816605	turquoise
EFEMP2	38639614,34335936,37982173,36819551	turquoise
ZNF217	33550903,26198954,21483406	turquoise
CAPG	32536029,29399702,26663173	turquoise
OCIAD2	39445005,39356352,27429853	turquoise
TRIP6	23339869,20876301,30061182	turquoise
PDIA4	35131603,33447054,32023222	turquoise
EGFR	31673738,37748218,32431518	grey
PARP9	36845744,36778644,32678519	turquoise
S100A13	34148033,20467443,32856232	turquoise
MSR1	37370848,35142109,33059718	turquoise
ADGRE5	38501000,37938973,34028660	turquoise
EMP3	38229014,37887529,34335936	turquoise
MMP14	35350840,38434278,34712139	turquoise
AEBP1	39315202,37730879,34988166	turquoise
PYGL	38293671,34177761,35037470	turquoise
MYBPH	39281062,37812190,35087137	turquoise
GPX7	38573391,35538763,35480989	turquoise
TGIF1	38573391,38372105,35569122	turquoise
SAA1	35800054,35756918,35574600	turquoise
CASP3	37195411,36329783,35601497	turquoise
RUNX1	39450533,38768760,36321611	turquoise
CHI3L1	38290591,37934565,37887529	turquoise
CD63	34377594,35966296,37928523	turquoise
PTX3	37439825,37781198,38359612	turquoise
TUBA1C	38577605,39355251,38396140	turquoise
PCOLCE	36882457,36882457,38533063	turquoise
MYD88	37456890,36778205,38847472	turquoise
ABCC3	34976054,34336837,38952353	turquoise
OTP	30257451,38499392,38952353	turquoise
RASSF10	31055025,20956940	grey
SLC7A7	36945359,23975734	turquoise
SLC16A3	38089757,27144334	turquoise
SLC2A4RG	30686753,28979815	turquoise
HOXC10	35845958,29179492	turquoise
RGS16	36414916,32319728	turquoise

LAPTM5	36945359,32582531	turquoise
UPP1	33498463,32583596	turquoise
F2RL2	37969372,32725165	turquoise
ARL9	35111661,32882327	turquoise
FAM20C	34970298,33239887	turquoise
FNDC3B	36275754,33336045	turquoise
TCIRG1	35266851,33664816	turquoise
FABP5	37114595,33837625	turquoise
FKBP10	33557829,34449972	turquoise
CNN3	35792226,34797350	turquoise
ELN	39539523,35127714	turquoise
ZDHHC12	35664705,35434031	turquoise
PTGFRN	35690717,35690717	turquoise
NNMT	35873494,35884600	turquoise
DIRAS3	36349462,35923699	turquoise
ERI1	36867360,36118697	turquoise
GALNT3	35565254,36539408	turquoise
PDPN	38825419,37093708	turquoise
S100A16	34148033,37151881	turquoise
PLOD3	34040895,37301776	turquoise
SOCS1	39654174,37315184	turquoise
LAMC1	38678297,37389756	turquoise
EN2	36061185,37432454	grey
RAB42	35741652,37698534	turquoise
IGFBP2	39633113,37737709	turquoise
STEAP3	39537233,37980651	turquoise
IGF2BP3	37180667,38029531	turquoise
BCAT1	33493139,38235619	turquoise
WEE1	39213054,38261152	turquoise
ADAM12	34638718,38272115	turquoise
CLIC1	34335936,38290591	turquoise
AQP1	38476871,38307919	grey
SLC43A3	38378721,38687049	turquoise
CALD1	39530009,39145081	turquoise
SMO	39084569,39457084	grey
CRISPLD1	18824526	turquoise
VOPP1	23243056	grey
ADAM33	23525950	turquoise
FGFRL1	24080485	turquoise
ENPP1	24531536	turquoise
AGBL2	24987500	grey
COL6A1	25325876	turquoise

DCTD	28912488	turquoise
G0S2	30388142	turquoise
ADAMTSL4	30728876	turquoise
PSPH	31861486	turquoise
ZYX	31949244	turquoise
PLK3	32065545	turquoise
WNT16	32181818	grey
DOK3	32193105	turquoise
AVIL	32651364	turquoise
ITPRIPL1	33550903	turquoise
ETV2	33732284	turquoise
COL5A2	34034744	turquoise
RHOC	34276990	turquoise
AP1S3	34367317	turquoise
GINS4	34556022	turquoise
CLCF1	35265072	turquoise
B3GNT7	35565254	turquoise
TNFRSF12A	35592520	turquoise
MAB21L2	35660939	grey
ACOT12	35986010	grey
FAM181A	36060266	turquoise
ARPC1B	36380368	turquoise
CASP5	36820395	turquoise
AK2	37161605	turquoise
RARRES2	37271257	turquoise
PSRC1	37326762	turquoise
LAMB4	37335645	turquoise
RCAN1	37918583	turquoise
PTPN7	37934565	turquoise
TENT5A	38204269	turquoise
VASN	38318849	turquoise
RBM47	38518642	turquoise
TIMP1	38603834	turquoise
MMP2	38720546	turquoise
F3	39006069	turquoise
ABRACL	39286126	turquoise
HEXB	39353936	turquoise
RDH5	39465792	turquoise
PDGFA	39606019	turquoise
CDC42BPG		grey
TGM5		grey
CNGA3		grey

FAM221A		grey
MGARP		grey
BANF2		grey
SLC28A1		grey
CFAP77		grey
ADGRD2		grey
RIPOR3		grey
KCTD19		grey
PLSCR2		grey
ESPNL		grey
FOXJ1		grey
FEZF1		grey
OCSTAMP		grey
SIX2		grey
DPY19L1		turquoise
COLGALT1		turquoise
BTG3		turquoise
TMEM106C		turquoise
TTYH3		turquoise
PABPC1L		turquoise
BEST4		turquoise
ANKRD53		turquoise
IGFLR1		turquoise
ECHDC2		turquoise
MCUB		turquoise
GAL3ST4		turquoise
PPM1M		turquoise
DNAH11		turquoise
C3orf52		turquoise
GPR157		turquoise
CD72		turquoise
CA3		turquoise
EMILIN1		turquoise
NFE2L3		turquoise
TEAD3		turquoise
CTF1		turquoise
PINLYP		turquoise
HDHD3		turquoise
TMEM154		turquoise
GRB14		turquoise
RINL		turquoise
CARD19		turquoise

TPRG1		turquoise
HEBP2		turquoise
FAM114A1		turquoise
MRC2		turquoise
BANK1		turquoise
SLFN12		turquoise
ALDH3A1		turquoise
FCHSD1		turquoise
RUBCNL		turquoise
CYTL1		turquoise
ARAP3		turquoise
PRICKLE3		turquoise

Table S7: Characteristics of the IDH1 wild type sample set.

	Highly methylated (n = 27)	Lowly methylated (n = 213)	P value	Lowly expressed (n = 30)	Highly expressed (n = 221)	P value
Histologic grade			<0.001[a]			<0.001[a]
LGG	26 (96.30%)	87 (40.85%)		30 (100%)	83 (37.56%)	
GBM	1 (3.70%)	126 (59.15%)		0 (0%)	138 (62.44%)	
Age	37.222 ±0.413	58.204 ±0.060	<0.001[b]	38.833 ±0.418	58.570 ±0.059	<0.001[b]
Gender			0.879[a]			0.388[a]
Male	15 (55.56%)	118 (55.40%)		16 (53.33%)	136 (61.54%)	
Female	12 (44.44%)	93 (43.66%)		14 (46.67)	85 (38.46%)	
Not reported	0 (0%)	2 (0.94%)		0 (0%)	0 (0%)	
Race			0.240[a]			0.812[a]
White	25 (92.59%)	170 (79.81%)		27 (90%)	197 (89.14%)	
Other	2 (7.41%)	32 (15.02%)		3 (10%)	21 (9.5%)	
Not reported	0 (0%)	11 (5.17%)		0	3 (1.36%)	
Ethnicity			0.016[a]			0.130[a]
Not hispanic or latino	22 (81.48%)	160 (75.12%)		25 (83.33%)	184 (83.26%)	
Hispanic or latino	3 (11.11%)	5 (2.35%)		3 (10%)	7 (3.17%)	
Not reported	2 (7.41%)	48 (22.54%)		2 (6.67%6.67%)	30 (13.57%)	
Vital status			<0.001[a]			<0.001[a]
Alive	24 (88.89%)	75 (35.21%)		27 (90%)	60 (27.15%)	
Dead	3 (11.11%)	136 (63.85%)		3 (10%)	161 (72.85)	
Not reported	0 (0%)	2 (0.94%)		0 (0%)	0 (0%)	
Overall survival (day)	2379	492	<0.001[c]	2379	454	<0.001[c]
	95%CI=2000-.	95%CI=428-561		95%CI=2000-.	95%CI=398-506	
MGMT promoter			<0.001[a]			<0.001[a]
Methylated	25 (92.59%)	82 (38.50%)		26 (86.67%)	70 (31.67%)	
Unmethylated	2 (7.41%)	126 (59.15%)		4 (13.33%)	122 (55.2%)	
Not reported	0 (0%)	5 (2.35%)		0 (0%)	29 (13.12%)	

[a], Chi-square test; [b], t tests; [c], Logrank test

References

Cao L, Li T, Ba Y, Chen E, Yang J, Zhang H (2022) Exploring Immune-Related Prognostic Signatures in the Tumor Microenvironment of Colon Cancer. Frontiers in Genetics 13. doi: 10.3389/fgene.2022.801484

Chen J, Lin Z, Barrett L, Dai L, Qin Z (2020) Identification of new therapeutic targets and natural compounds against diffuse intrinsic pontine glioma (DIPG). Bioorg Chem 99: 13.

Gatto F, Ferreira R, Nielsen J (2020) Pan-cancer analysis of the metabolic reaction network. Metabolic Engineering 57: 51-62. doi: https://doi.org/10.1016/j.ymben.2019.09.006

Hervás-Corpión I, Gallardo-Orihuela A, Catalina-Fernández I, Iglesias-Lozano I, Soto-Torres O, Geribaldi-Doldán N, Domínguez-García S, Luna-García N, Romero-García R, Mora-López F, Iriarte-Gahete M, Morales JC, Campos-Caro A, Castro C, Gil-Salú JL, Valor LM (2021) Potential Diagnostic Value of the Differential Expression of Histone H3 Variants between Low- and High-Grade Gliomas. Cancers 13.

Kaisman-Elbaz T, Elbaz Y, Merkin V, Dym L, Noy A, Atar-Vardi M, Bari R, Turiel S, Alt A, Zamed T, Eskira Y, Lavrenkov K, Kezerle Y, Dyomin V, Melamed I (2020) Hemoglobin Levels and Red Blood Cells Distribution Width Highlights Glioblastoma Patients Subgroup With Improved Median Overall Survival. Front Oncol 10.

Kim YW, Koul D, Kim SH, Lucio-Eterovic AK, Freire PR, Yao J, Wang J, Almeida JS, Aldape K, Yung WK (2013) Identification of prognostic gene signatures of glioblastoma: a study based on TCGA data analysis. Neuro Oncol 15: 829-39.

Li Z, Cui Y, Duan Q, Zhang J, Shao D, Cao X, Gao Y, Wang S, Li J, Jones OD, Lei X, Wang L, Zhou X, Xu M, Ma J, Liu Y, Xu X (2022) The Prognostic Significance of FKBP1A and Its Related Immune Infiltration in Liver Hepatocellular Carcinoma. Int J Mol Sci 23.

Meza-Zepeda LA, Forus A, Lygren B, Dahlberg AB, Godager LH, South AP, Marenholz I, Lioumi M, Flørenes VA, Maelandsmo GM, Serra M, Mischke D, Nizetic D, Ragoussis J, Tarkkanen M, Nesland JM, Knuutila S, Myklebost O (2002) Positional cloning identifies a novel cyclophilin as a candidate amplified oncogene in 1q21. Oncogene 21: 2261-9.

Park ER, Kim SB, Lee JS, Kim YH, Lee DH, Cho EH, Park SH, Han CJ, Kim BY, Choi DW, Yoo YD, Yu A, Lee JW, Jang JJ, Park YN, Suh KS, Lee KH (2017) The mitochondrial hinge protein, UQCRH, is a novel prognostic factor for hepatocellular carcinoma. Cancer Med 6: 749-760.

Shen Z, Feng X, Fang Y, Li Y, Li Z, Zhan Y, Lin M, Li G, Ding Y, Deng H (2019) POTEE drives colorectal cancer development via regulating SPHK1/p65 signaling. Cell Death & Disease 10: 863. doi: 10.1038/s41419-019-2046-7

Wang J, Huang F, Zhao J, Huang P, Tan J, Huang M, Ma R, Xiao Y, He S, Wang Z, Shen J, Lu H, Meng L (2022) Tumor-Infiltrated CD8+ T Cell 10-Gene Signature Related to Clear Cell Renal Cell Carcinoma Prognosis. Front Immunol 13.

Wang L, Li M, Zhan Y, Ban X, Zeng T, Zhu Y, Yun J, Guan XY, Li Y (2018) Down-regulation of POTEG predicts poor prognosis in esophageal squamous cell carcinoma patients. Mol Carcinog 57: 886-895.

Wang S, Li M, Xing L, Yu J (2019) High expression level of peptidylprolyl isomerase A is correlated with poor prognosis of liver hepatocellular carcinoma. Oncol Lett 18: 4691-4702. doi: 10.3892/ol.2019.10846

Zhang K, Sun L, Kang Y (2023) Regulation of phosphoglycerate kinase 1 and its critical role in cancer. Cell Communication and Signaling 21: 240. doi: 10.1186/s12964-023-01256-4

Zhang L, Zhao Q, Mao L, Li H, Zhuang M, Wang J, Liu Y, Qi M, Du X, Xia Z, Sun N, Liu Q, Chen H, Zhang R (2021) Bioinformatics Analyses Reveal the Prognostic Value and Biological Roles of SEPHS2 in Various Cancers. Int J Gen Med 14: 6059-6076.

Zhou J, Xing Z, Xiao Y, Li M, Li X, Wang D, Dong Z (2022) The Value of H2BC12 for Predicting Poor Survival Outcomes in Patients With WHO Grade II and III Gliomas. Front Mol Biosci 9.